

An essential role for the MAL protein in targeting Lck to the plasma membrane of human T lymphocytes

Olga Antón,¹ Alicia Batista,¹ Jaime Millán,¹ Laura Andrés-Delgado,¹ Rosa Puertollano,² Isabel Correas,¹ and Miguel A. Alonso¹

¹Centro de Biología Molecular "Severo Ochoa," Consejo Superior de Investigaciones Científicas, Universidad Autónoma de Madrid, 28049 Madrid, Spain

²Laboratory of Cell Biology, National Heart, Lung, and Blood Institute, National Institutes of Health, Bethesda, MD 20892

The MAL protein is an essential component of the specialized machinery for apical targeting in epithelial cells. The src family kinase Lck plays a pivotal role in T cell signaling. We show that MAL is required in T cells for efficient expression of Lck at the plasma membrane and activation of *IL-2* transcription. To investigate the mechanism by which MAL regulates Lck targeting, we analyzed the dynamics of Lck and found that it travels to the plasma membrane in specific transport carriers containing MAL. Coimmunoprecipitation experiments indicated an association of MAL with Lck. Both carrier formation and partitioning of Lck into detergent-insoluble membranes were ablated in the absence of MAL. Polarization of T cell receptor for antigen (TCR) and microtubule-organizing center to immunological synapse (IS) were also defective. Although partial correction of the latter defects was possible by forced expression of Lck at the plasma membrane, their complete correction, formation of transport vesicles, partitioning of Lck, and restoration of signaling pathways, which are required for *IL-2* transcription up-regulation, were achieved by exogenous expression of MAL. We concluded that MAL is required for recruitment of Lck to specialized membranes and formation of specific transport carriers for Lck targeting. This novel transport pathway is crucial for TCR-mediated signaling and IS assembly.

CORRESPONDENCE

Miguel A. Alonso:
maalonso@cbm.uam.es

Abbreviations used: IS, immunological synapse; JTIM, Jurkat TCR-signaling impaired mutant; mRNA, messenger RNA; MTOC, microtubule-organizing center; SEE, staphylococcal enterotoxin E; siRNA, short interfering RNA.

Induction of tyrosine phosphorylation by the TCR is essential for proliferation and differentiation of resting T cells into effector cells. One of the earliest intracellular modifications of downstream TCR recognition is the activation of the src family kinase Lck, which phosphorylates tyrosine residues of CD3, ZAP-70, and other substrates that initiate signaling cascades leading to T cell activation and proliferation (1). In the absence of Lck, the TCR fails to induce any tyrosine phosphorylation and all downstream signaling events are blocked (2, 3). Lck is predominantly associated with the cytosolic side of the plasma membrane, a localization which is consistent with its importance in the early signaling events involving the TCR (4). The N-terminal Gly-Cys-Val-Cys sequence of Lck is modified by the addition of myristate and palmitate to the glycine and the two cysteine residues, respectively (5). Transport of Lck

to the plasma membrane relies on the exocytic pathway (6) and requires acylation of its N-terminal sequence (7). Lck acylation is also essential for activation of downstream signaling pathways (7) and partitioning into detergent-resistant membranes (5) that are postulated to contain specialized membrane microdomains (8). Given the importance of Lck, the characterization of the cellular and molecular mechanisms that govern its transport to the plasma membrane is essential for understanding its function and dynamics. Although much is known about the biochemical regulation of Lck, very little is known about the protein machinery involved in the targeting of Lck to the T cell plasma membrane.

MAL is a 17-kD integral membrane protein containing a MARVEL (MAL and related proteins for vesicle trafficking and membrane link)

© 2008 Antón et al. This article is distributed under the terms of an Attribution-Noncommercial-Share Alike-No Mirror Sites license for the first six months after the publication date (see <http://www.jem.org/misc/terms.shtml>). After six months it is available under a Creative Commons License (Attribution-Noncommercial-Share Alike 3.0 Unported license, as described at <http://creativecommons.org/licenses/by-nc-sa/3.0/>).

O. Antón and A. Batista contributed equally to this paper.

domain present in proteins associated with membrane juxtaposition events (9) such as synaptophysins, synaptogyrins, and occludin (9). The MAL cDNA, which was initially characterized as being differentially expressed in Jurkat cells and other T cell lines, but not in B cell lines (10), is also expressed in polarized epithelial cells. MAL is selectively detected in detergent-resistant membrane fractions of epithelial cells, Jurkat cells, and PBLs (11, 12). Although the function of MAL in epithelial cells as an essential component of the machinery for specialized protein exocytosis to the apical surface is well established (12–14), its function in T cells has remained merely a matter of speculation (15).

In response to appropriate antigens presented by an APC, TCR-induced signals assemble a sophisticated apparatus for ongoing signaling (1) and induce T cells to polarize and form a surface subdomain at the T cell–APC contact zone, known as the immunological synapse (IS) (16). The formation of an IS is a dynamic process that involves polarization of TCR, Lck, and other signaling machinery, microtubule-organizing center (MTOC), integrin LFA-1, and actin cytoskeleton (16). The Jurkat T cell line and mutant derivatives have been important tools for investigating TCR-driven signaling and polarization (17). In this study, we have used MAL knockdown experiments involving short interfering RNA (siRNA) expression in Jurkat cells and primary T lymphocytes and a novel TCR signaling-defective Jurkat cell clone lacking MAL expression to investigate the role of MAL in T cells. Time-lapse videomicroscopy showed that Lck reaches the plasma membrane in transport carriers containing MAL. The formation of the carriers, as well as the partitioning of Lck into detergent-resistant membranes, was blocked in the absence of MAL expression, resulting in intracellular accumulation of Lck. The formation of transport carriers for Fyn or p75 was not affected under those conditions. Probably as a consequence of the depletion of Lck at the plasma membrane, polarized assembly of TCR and Lck to the IS and activation of the signaling pathways leading to IL-2 gene transcription were both impaired. Exogenous expression of MAL fully corrects all the functional defects observed in the absence of MAL expression including formation of Lck transport carriers, partitioning of Lck, and IL-2 promoter activation. Therefore, MAL, which was found to associate with Lck, has an essential role mediating the targeting of Lck to the T cell plasma membrane by allowing recruitment of Lck to specialized intracellular membrane microdomains and formation of specific transport carriers destined for the plasma membrane. This novel transport pathway is crucial for TCR-mediated signaling and IS formation.

RESULTS

Polarized targeting to the IS is deficient when MAL is not expressed

During a screening program involving the analysis of cDNA microarrays to identify novel Jurkat T cell mutants with defective TCR-induced signaling, a cell clone known as Jurkat TCR-signaling impaired mutant (JTIM) with no detectable MAL messenger RNA (mRNA) expression was isolated.

The procedure used was similar to that previously described for the generation and selection of mutants defective in PMA-induced CD69 up-regulation (18, 19). The reduced MAL mRNA expression in this clone was further confirmed by Northern blot and quantitative RT-PCR analyses (Fig. S1, A and B, available at <http://www.jem.org/cgi/content/full/>

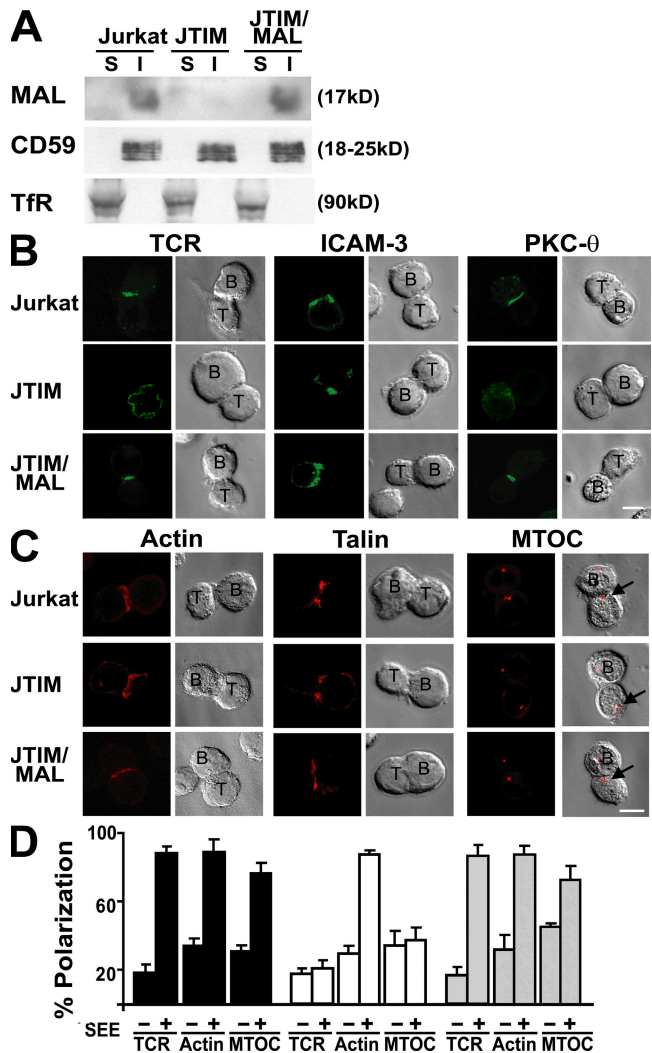


Figure 1. MAL expression is required for translocation of TCR and reorientation of MTOC to IS. (A) Normal Jurkat cells, JTIM cells, and JTIM/MAL cells were extracted with 1% Triton X-100 at 4°C. The soluble (S) and insoluble (I) fractions were isolated by centrifugation to equilibrium in sucrose density gradients. Equivalent aliquots from both fractions were analyzed by immunoblotting with anti-MAL mAb 6D9. The distributions of CD59 and Tfr, as respective markers of the insoluble and soluble fractions, were analyzed as a control of the fractionation procedure. (B and C) Cells were conjugated to SEE-pulsed APCs for 15 min. After cell fixation, the distribution of TCR, ICAM-3, and PKC-θ (B) and that of actin, talin, and γ-tubulin (C) were analyzed in nonpermeabilized or permeabilized cells, respectively. The arrows indicate the position of the MTOC in the T cell. (D) The mean percentage ± SEM of Jurkat cells in T cell–APC conjugates with polarized distribution of TCR, actin, and MTOC to the IS was quantified in three independent experiments. $n > 100$ T cells/experiment (right). Bars, 5 μm.

jem.20080552/DC1). Fig. 1 A confirms that JTIM cells do not express detectable levels of MAL, whereas the expression of MAL and its partition in detergent-insoluble membrane fractions were similar in normal Jurkat cells and JTIM cells in which MAL expression was reconstituted by stable transfection of MAL cDNA (JTIM/MAL cells). JTIM cells established T cell–APC conjugates either in the presence or absence of staphylococcal enterotoxin E (SEE) superantigen with the same efficiency as normal Jurkat cells (Fig. S1C), allowing investigation of the possible requirement of MAL for targeting of receptors, cytoskeleton, and signaling molecules to IS. JTIM cells were unable to translocate the TCR, PKC-

θ, and MTOC to the IS in response to stimulation, whereas ICAM-3, actin, and talin distributed to the IS normally (Fig. 1, B–D). In addition, JTIM cells failed to target ZAP-70 and LAT to the IS (Fig. S2). It is of particular note that stable exogenous expression of MAL in JTIM cells restored the IS polarization pattern observed in normal Jurkat cells (Fig. 1, B–D and Fig. S2).

To confirm that MAL is required for normal IS formation, we used an RNA interference knockdown approach. For this purpose, we expressed siRNAs (MAL siRNA1 and 2) targeted to a region adjacent to the AUG translation initiation site (MAL siRNA1) or to the 3' untranslated region

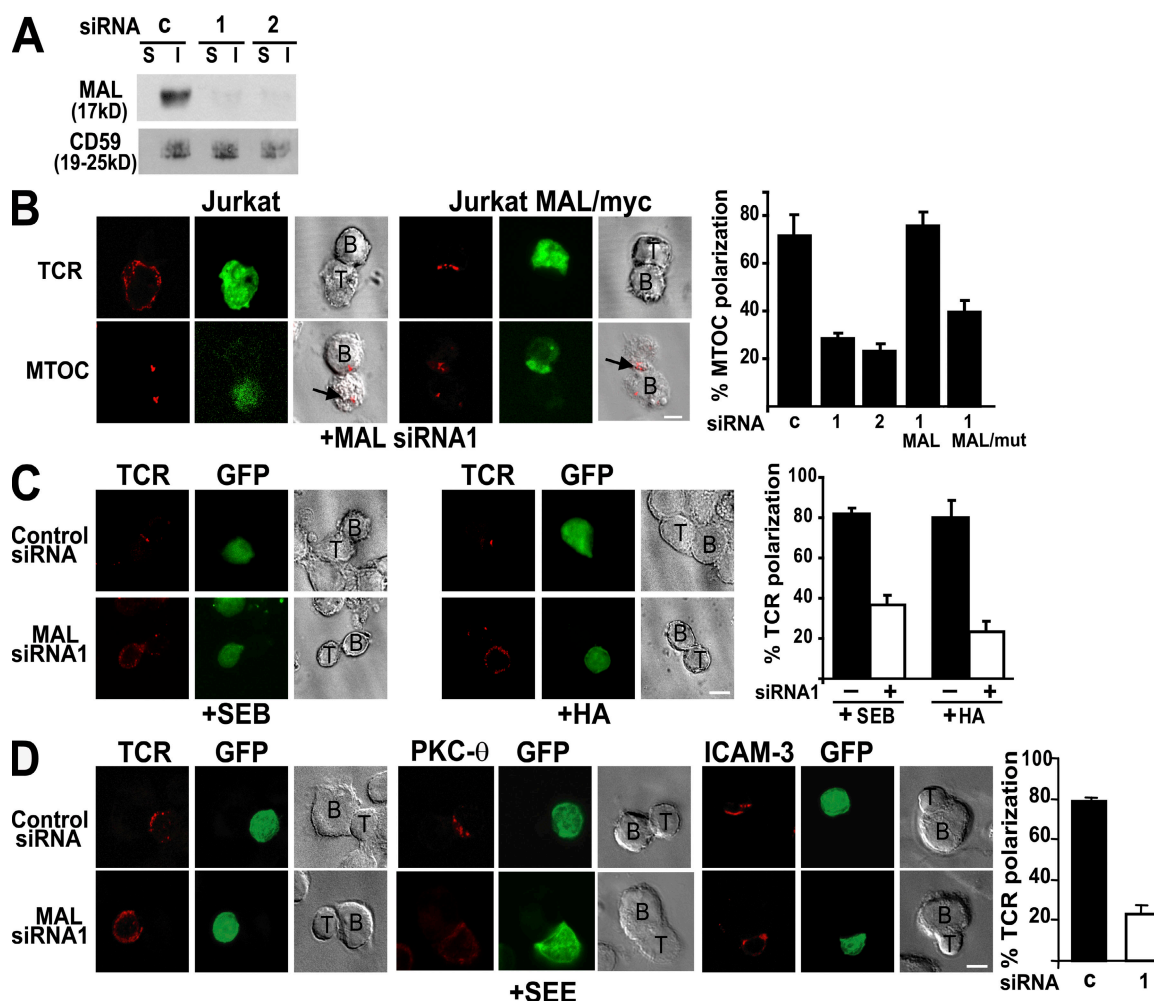


Figure 2. Effect of MAL knockdown on IS formation in Jurkat cells and primary T lymphocytes. (A) Jurkat cells were transfected with DNA constructs expressing GFP and a control (c) siRNA or the indicated MAL siRNA and incubated for 48 h at 37°C. GFP-expressing cells were separated in a cell sorter and analyzed for MAL expression by immunoblotting with anti-MAL mAb 6D9. (B) Normal Jurkat cells or Jurkat cells stably expressing either MAL/myc or MALmut/myc were transfected with pMAL-siRNA1/GFP or pMAL-siRNA2/GFP, as indicated. After 48 h at 37°C, cells were conjugated to SEE-loaded Raji cells for 20 min and fixed. The distribution of TCR and MTOC was determined by immunofluorescence analysis. The arrows indicate the position of the MTOC in the T cell. A quantitative analysis of the effect of MAL siRNA expression on MTOC reorientation is shown in the histogram. (C) Jurkat CH7C17 cells expressing GFP and a control siRNA or MAL siRNA1 for 48 h at 37°C were conjugated to either SEB or HA peptide-loaded HOM2 cells for 20 min and fixed. The distribution of TCR was determined by immunofluorescence analysis. (D) Human PBLs were transfected with plasmid DNA expressing GFP and a control siRNA or MAL siRNA1 and incubated for 36 h at 37°C. Cells were then conjugated to SEE-loaded APCs for 15 min. After cell fixation, the distribution of TCR, PKC-θ, and ICAM-3 was determined by immunofluorescence analysis. The histograms show the mean ± SEM of the percentage of APC-conjugated GFP-expressing T cells with MTOC (B) or TCR (C and D) polarized to the IS. Three independent experiments were performed. $n > 100$ T cells/experiment. Bars, 5 μ m.

(MAL siRNA2) of endogenous human MAL mRNA. To identify the transfected cell population, GFP was expressed from the same DNA constructs. Expression of MAL siRNA1 and 2 was able to reduce endogenous MAL levels of Jurkat cells to <10% of the MAL content in cells expressing a control siRNA (Fig. 2 A). MAL knockdown in Jurkat cells recapitulated the IS targeting defects observed in JTIM cells for TCR and MTOC (Fig. 2 B), as well as for PKC- θ (not depicted). To rule out possible spurious effects of the siRNA, we used a stable clone of Jurkat cells (Jurkat MAL/myc cells) expressing MAL, tagged at its amino terminus with the Myc epitope encoded by a recombinant mRNA that does not fully pair with MAL siRNA1 (12). The expression of MAL siRNA1 in these cells had no effect on the polarization of TCR and MTOC to the IS because the exogenous protein was able to substitute the endogenous protein (Fig. 2 B). As a further control we observed that the expression of a similar MAL protein (MALmut/myc) with a modified sequence at its carboxyl terminus (RWKSS→RWSSS), which is known to be inactive in polarized apical transport (20), was unable to replace endogenous MAL (Fig. 2 B, histogram).

It is apparent that the effect of MAL depletion on IS targeting was not restricted to the use of the superantigen SEE, given that similar results were observed in T cell–APC conjugates formed with Jurkat CH7C17 cells (21) in the presence of staphylococcal enterotoxin B or the influenza HA peptide 307–319 (Fig. 2 C). Similar to the case of MAL-deficient Jurkat cells, expression of MAL siRNA in primary T lymphocytes resulted in an impaired translocation of TCR and PKC- θ , but not of ICAM-3, to the IS (Fig. 2 D). Thus, using Jurkat cells and primary T lymphocytes, we observed that normal IS formation is strictly dependent on MAL expression.

MAL is required for the targeting of Lck to the plasma membrane

In an attempt to identify proteins whose surface expression might be affected in JTIM cells, we analyzed the plasma membrane distribution of TCR, ICAM-3, LAT, CD4, CD28, LFA-1, glycosylphosphatidylinositol-anchored proteins (CD59 and CD55), and Lck at steady state. Among the molecules examined, there were proteins mostly detected in detergent-insoluble membranes of resting T cells (LAT, CD59, CD55, and Lck) or predominantly excluded from these membrane fractions (TCR, ICAM-3, CD4, CD28, and LFA-1). Only in the case of Lck did we observe striking differences in distribution between MAL-deficient and MAL-expressing Jurkat cells. Thus, although Lck was distributed at the cell periphery and in internal endosome structures in WT Jurkat and JTIM/MAL cells, it was present only at very low levels at the plasma membrane and was largely concentrated in a compact intracellular structure in most JTIM cells (Fig. 3 A). Consistent with the intracellular accumulation observed in JTIM cells, MAL siRNA expression diminished the expression of Lck at the cell periphery and led to its intracellular accumulation also in primary T lymphocytes (Fig. 3 B). It is of particular note that the loss of peripheral Lck in JTIM cells was associated

with the predominant exclusion of Lck from detergent-insoluble membranes (Fig. 3 C). This implies that MAL expression in Jurkat cells is necessary for both efficient Lck targeting to the plasma membrane and normal partitioning into detergent-insoluble membrane fractions. Neither the partitioning of LAT (Fig. 3 C) and CD59 (Fig. 1 A) nor their targeting at the cell surface was affected by the absence of MAL (Fig. S2 and not depicted). Pulse-chase experiments revealed that although Lck was already associated with membranes in normal and JTIM cells 15 min after its biosynthesis, incorporation of Lck into detergent-insoluble membranes was only observed in normal cells (Fig. S3). As occurred with the TCR, Lck did not redistribute to the IS in T cell–APC conjugates formed using JTIM cells (Fig. 3 D). The observation that the levels of Lck into detergent-insoluble membranes strictly correlated with MAL expression prompted us to analyze whether MAL associates with Lck. Coimmunoprecipitation experiments using Jurkat MAL/myc cells indicated association of MAL with endogenous Lck (Fig. 3 E, left). This association was also detected in COS-7 cells transiently expressing both proteins (Fig. 3 E, right). The interaction was mapped to the amino terminus of Lck, as demonstrated by coimmunoprecipitation of MAL with a chimera consisting of the membrane proximal 10-aa sequence of Lck fused to GFP (Lck₁₀-GFP). As controls, we observed that neither the p75-GFP chimera nor GFP coimmunoprecipitated with MAL (Fig. 3 E, right).

To address whether impaired IS assembly in JTIM cells was caused by the low levels of Lck at the cell periphery, JTIM cells were forced to express Lck at the plasma membrane by transfecting DNA constructs encoding CD4/Lck or LAT/Lck chimeras, consisting of the extracellular and transmembrane domains of mouse CD4 or human LAT, respectively, fused to the amino terminus of Lck. The use of the CD4 and LAT transmembrane domains, which are predominantly excluded from or associated with detergent-insoluble membranes, respectively, allowed us to investigate whether the partitioning of Lck in this type of membrane influences IS formation in the absence of MAL expression. Fig. 4 (A–C) shows that the expression of either chimera in JTIM cells bypassed the requirement of MAL for targeting TCR, ZAP-70, and PKC- θ , but not the MTOC, to the IS. Furthermore, the chimeras were unable to rescue Erk activation (Fig. 4 D), which was deficient in JTIM cells, and CD69 up-regulation (Fig. 4 E), which is regulated by transcription factor AP-1, in response to stimulation.

In summary, these data show that MAL regulates the targeting of Lck to the plasma membrane, probably by allowing its inclusion in specialized membrane microdomains and that, although the absence of Lck at the plasma membrane is likely to be a major cause of the defects observed in MAL-depleted cells, it is not the sole cause because forced expression of Lck to the plasma membrane was not able to restore all the defects.

MAL is necessary for the formation of vesicular carriers that transport Lck to the plasma membrane

The requirement of MAL for Lck targeting to the T cell surface prompted us to compare the distribution of these two

molecules in Jurkat cells. As our anti-MAL mAb is not of use in immunofluorescence analysis, we used Jurkat cells stably expressing GFP-MAL. Confocal microscopic analysis shows that MAL and Lck colocalized extensively at these two locations (Fig. 5 A). Next, we studied the dynamics to investigate the possible involvement of MAL in Lck transport using a Lck-GFP chimera. As a control, we observed that transiently expressed Lck-GFP accumulated intracellularly in JTIM cells even more drastically than endogenous Lck, whereas Lck-GFP was able to reach the plasma membrane efficiently in

normal Jurkat and JTIM/MAL cells (Fig. 5 B). To trace the formation and movement of Lck transport vesicles from the perinuclear region to the cell surface in living cells and to compare Lck dynamics with those of MAL, we transiently expressed Lck-Cherry in Jurkat cells stably expressing GFP-MAL. The presence of the fluorescent protein moiety in MAL and Lck did not affect either their partitioning into detergent-insoluble membranes or their subcellular distribution (unpublished data). Time-lapse experiments showed that MAL and Lck travel in the same transport carriers destined for the

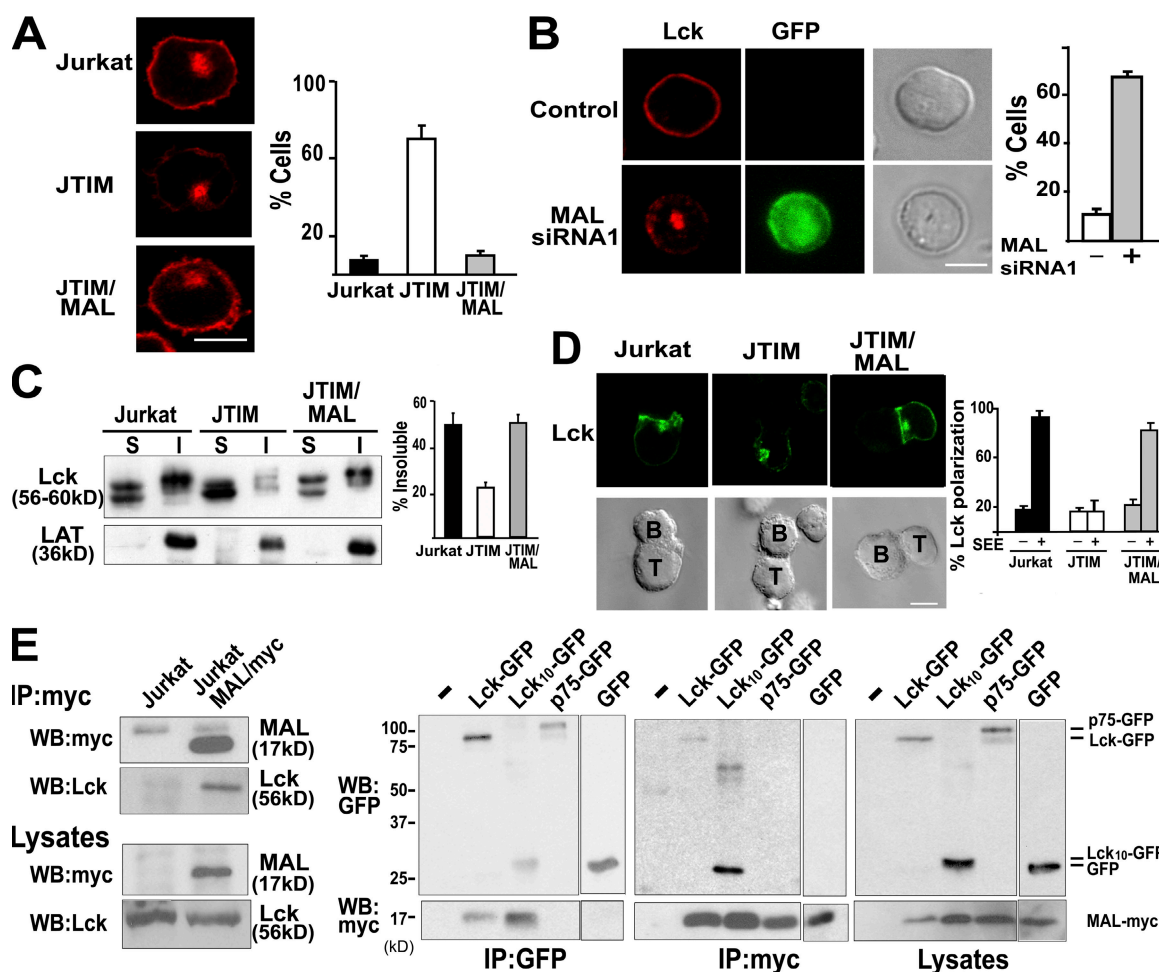


Figure 3. MAL is required for the targeting of Lck to the plasma membrane. (A) The subcellular distribution of endogenous Lck was analyzed by indirect immunofluorescence in the three types of Jurkat cell. The percentage of cells with low levels of peripheral Lck are shown on the right and measured as described in Materials and methods. (B) Human PBLs were transfected with plasmid DNA expressing GFP and MAL siRNA1 and incubated for 36 h at 37°C. After cell fixation, the distribution of Lck was determined by immunofluorescence analysis in three independent experiments. $n > 100$ T cells/experiment. The histograms represent the mean percentage \pm SEM of cells with predominant intracellular localization of Lck. (C) The soluble (S) and insoluble (I) membrane fractions of resting normal Jurkat cells, JTIM cells, and JTIM/MAL cells were isolated by centrifugation to equilibrium. Equivalent aliquots from both fractions were then analyzed by immunoblotting to detect endogenous Lck and LAT. The histogram represents the mean percentage \pm SEM of Lck into the membrane insoluble fraction. Three independent experiments were performed. (D) Cells were conjugated to SEE-pulsed APCs for 15 min. After cell fixation, the distribution of Lck was analyzed. The histogram represents the mean percentage of Jurkat cells in T cell-APC conjugates with polarized distribution of Lck to the IS as quantified in three independent experiments. $n > 100$ T cells/experiment. (E) Lysates of normal Jurkat cells or Jurkat cells stably expressing MAL/myc cells were immunoprecipitated with anti-myc mAb, and the immunoprecipitates and the original lysates were analyzed by immunoblotting with antibodies to the c-myc tag or to Lck as indicated (left). Normal COS-7 cells or COS-7 cells transiently coexpressing MAL/myc and Lck-GFP, Lck₁₀-GFP, p75-GFP, or GFP were lysed and immunoprecipitated with anti-myc or GFP antibodies. The immunoprecipitates and the original lysates were finally analyzed by immunoblot with anti-myc and anti-GFP antibodies as indicated (right). Bars, 5 μ m.

plasma membrane (Fig. 5 C and Video 1, available at <http://www.jem.org/cgi/content/full/jem.20080552/DC1>). The colocalization plot of MAL and Lck shows a high level of colocalization between both proteins throughout the time-lapse experiment. The Pearson's correlation coefficient and the overlap coefficient according to Manders (22) were 0.945 and 0.954, respectively.

To examine the requirement of MAL for the formation of the Lck transport vesicles, we compared the dynamics of Lck at the perinuclear accumulation in the three types of Jurkat cell. Fig. 6 A and Videos 2–4 (available at <http://www>

[jem.org/cgi/content/full/jem.20080552/DC1](http://www.jem.org/cgi/content/full/jem.20080552/DC1)) show that although formation of Lck exocytic vesicles occurred in MAL-expressing cells, this process was almost completely blocked in JTIM cells. Only a very small number of much smaller vesicles were sporadically detected in JTIM cells. As a control, we observed that JTIM cells, although unable to transport Lck to the plasma membrane, were active in the formation of transport vesicles containing the transmembrane protein p75 or the tyrosine kinase Fyn (Fig. 6 B and Videos 5 and 6). Consistent with these observations, unlike MAL and Lck, which colocalized extensively, Fyn and p75 showed a much

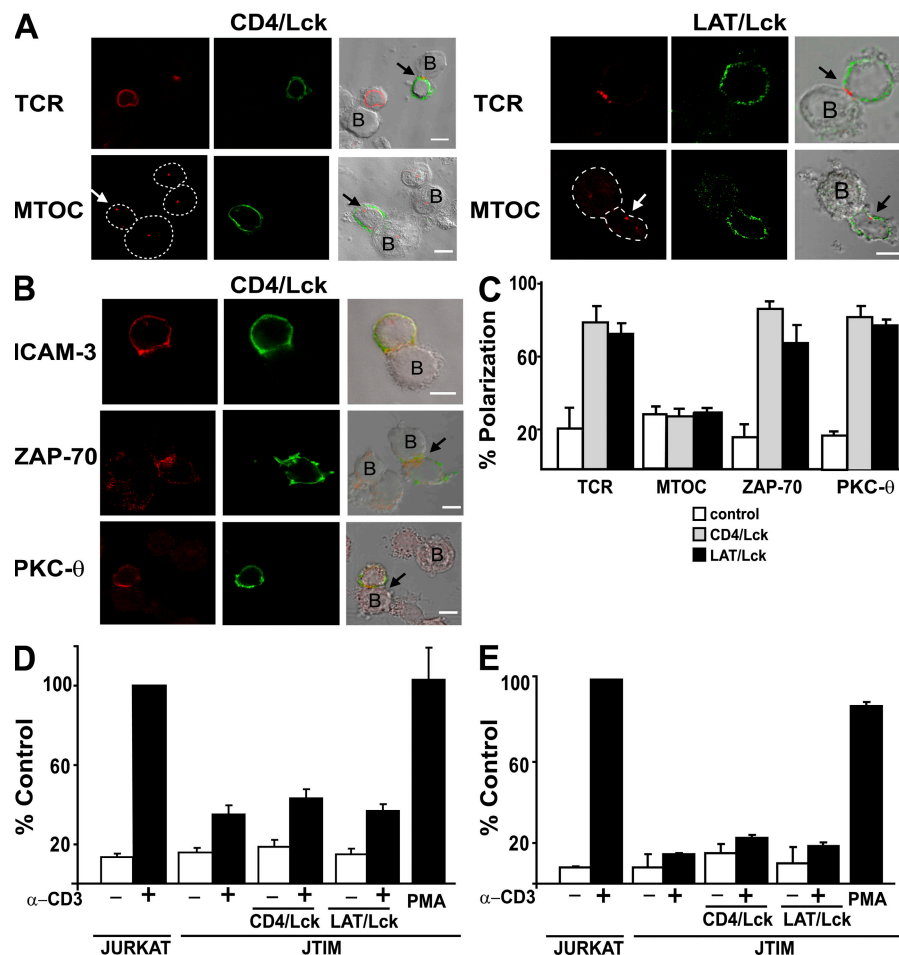


Figure 4. Forced expression of Lck at the plasma membrane in MAL-deficient cells corrects TCR targeting to the IS. JTIM cells were transfected with the CD4/Lck or the LAT/Lck plasmids. After 48 h at 37°C, cells were conjugated to SEE-loaded Raji cells for 20 min and fixed. Transfected cells were detected with antibodies to mouse CD4 or to the c-Myc tag to detect expression of the CD4/Lck or LAT/Lck chimeras, respectively. (A) The distribution of TCR and MTOC was determined by immunofluorescence analysis. In the case of MTOC analysis, the contour of the cells has been drawn with a dotted line to facilitate the identification of the cells. The arrows indicate the position of the TCR or MTOC in the T cells expressing the chimera. (B) The distribution of ICAM-3, ZAP-70, and PKC-θ was determined by immunofluorescence analysis. Conjugates in A and B formed by untransfected JTIM cells serve as internal controls. Bars, 5 μm. (C) Quantitative analysis of the polarization of TCR, MTOC, ZAP-70, and PKC-θ in JTIM cells expressing the CD4/Lck or LAT/Lck chimeras. Three independent experiments were performed. $n > 100$ T cells/experiment. The histogram shows the mean percentage \pm SEM of APC conjugates with TCR, MTOC, ZAP-70, or PKC-θ polarized to the IS. (D and E) Jurkat cells and JTIM cells transfected or not with the CD4/Lck or LAT/Lck chimeras were transfected with CD4ΔCyt-GFP (D) or pEGFP-C1 (E) and treated with activating anti-CD3 antibodies or PMA as indicated. After 15 min (D) or 16 h (E) at 37°C, EGFP-expressing cells were analyzed for phosphorylated Erk (D) or CD69 (E) expression by flow cytometry. The cotransfection efficiency was $>80\%$ as determined by immunofluorescence microscopy. The histograms show the percentage \pm SEM of the mean fluorescence of phospho-Erk and CD69 obtained in each case relative to that of Jurkat cells stimulated with anti-CD3 antibodies. Three independent experiments were performed.

lower colocalization with MAL (Fig. 6 C). The Pearson's correlation coefficient and the overlap coefficient according to Manders were 0.710 and 0.740, respectively, for MAL/

p75 and 0.752 and 0.546 for MAL/Fyn. We conclude from this set of experiments that MAL colocalizes extensively with Lck at steady state, is present in the same transport carriers that contain Lck, and is essential for the formation of such specific carriers.

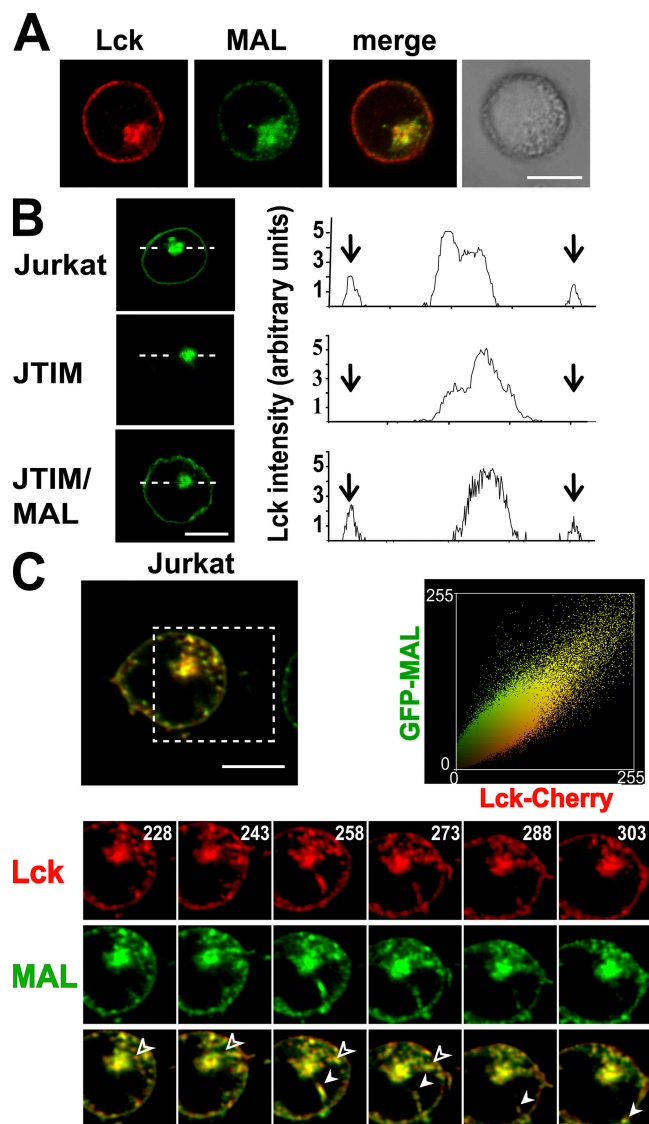


Figure 5. Lck and MAL travel in the same transport vesicles destined for the plasma membrane. (A) Jurkat cells stably expressing GFP-MAL were subjected to double label immunofluorescence analysis to detect GFP-MAL and endogenous Lck. (B) Cells were transfected with Lck-GFP and the distribution of Lck-GFP was analyzed 20 h later. A densitometric analysis of the distribution of Lck-GFP along the line in each type of cell is shown on the right panels. Arrows indicate the position of the periphery of the cell. (C) Jurkat cells stably expressing GFP-MAL were transiently transfected with plasmid DNA expressing Lck-Cherry and subjected to time-lapse videomicroscopy. The processes occurring within the region indicated by the dashed square are shown at higher magnification in the bottom panels. Solid and empty arrowheads indicate two vesicles transporting MAL and Lck together to the plasma membrane. Numbers indicate time in seconds. The plot on the right shows a high correlation of the colocalization of MAL and Lck throughout the time-lapse experiment (Pearson's correlation coefficient = 0.945).

MAL is essential for activation-induced AP-1, NF- κ B, and NFAT activities and for tyrosine phosphorylation in Jurkat cells

Because the JTIM cell clone was isolated as defective in TCR-mediated signaling, we investigated whether exogenous expression of MAL rescued the signaling defect by analyzing the effect of MAL expression in various signaling cascades induced by TCR stimulation. We first compared the activation of the mitogen-activated protein kinase Erk, p38, and JNK pathways, which lead to increased AP-1 activity, in the three Jurkat cell systems used that were stimulated with SEE (Fig. 7 A, left). Erk activation was detected in normal Jurkat cells but not in JTIM cells. Reconstitution of MAL in JTIM cells rescued Erk activation. In contrast to Erk, activation of p38 and JNK kinases was less affected in JTIM cells. Because AP-1 activity is regulated by Erk, JTIM cells were, as expected, deficient in their ability to stimulate AP-1 activity (Fig. 7 A, right). The activation state of the NF- κ B pathway was examined by analyzing the phosphorylation of the IKK- α/β subunits of IKK, a hallmark of the NF- κ B activation pathway (Fig. 7 B, left). Similar to the case of Erk, JTIM cells were unable to induce IKK- α/β phosphorylation, whereas normal phosphorylation occurred in JTIM/MAL cells. The impairment of IKK- α/β phosphorylation in JTIM, but not in WT Jurkat or MAL-expressing JTIM cells, was associated with the inhibition of NF- κ B activity (Fig. 7 B, right). The functionality of the NFAT activation pathway was addressed by analyzing the dephosphorylation of NFAT, which is a step required for NFAT activation (Fig. 7 C, left). This process was equally functional in normal Jurkat cells and JTIM/MAL cells even though it did not occur in JTIM cells. Consistent with this result, induction of NFAT transcriptional activity was impaired in JTIM cells compared with observations in the two types of MAL-expressing Jurkat cell (Fig. 7 C, right). Finally, we noticed that tyrosine phosphorylation of CD3 ζ , ZAP-70, and PLC- γ 1 in response to stimulation was defective in the absence of MAL but normal in the two types of MAL-expressing Jurkat cell, even though the three types of Jurkat cell that we used expressed similar levels of the three proteins (Fig. 7 D).

Next, we analyzed whether, in addition to restoring AP-1, NF- κ B, and NFAT responses to stimulation, exogenous MAL expression in JTIM cells was able to do the same with the transcriptional activation of the IL-2 promoter. Fig. 7 E shows that JTIM/MAL cells responded to SEE stimulation by activating IL-2 promoter-driven transcription at levels similar to those of normal Jurkat cells, whereas JTIM cells were basically unresponsive. As a control, we observed that all three cells were able to respond to stimulation with PMA plus ionomycin, indicating that this treatment bypasses the

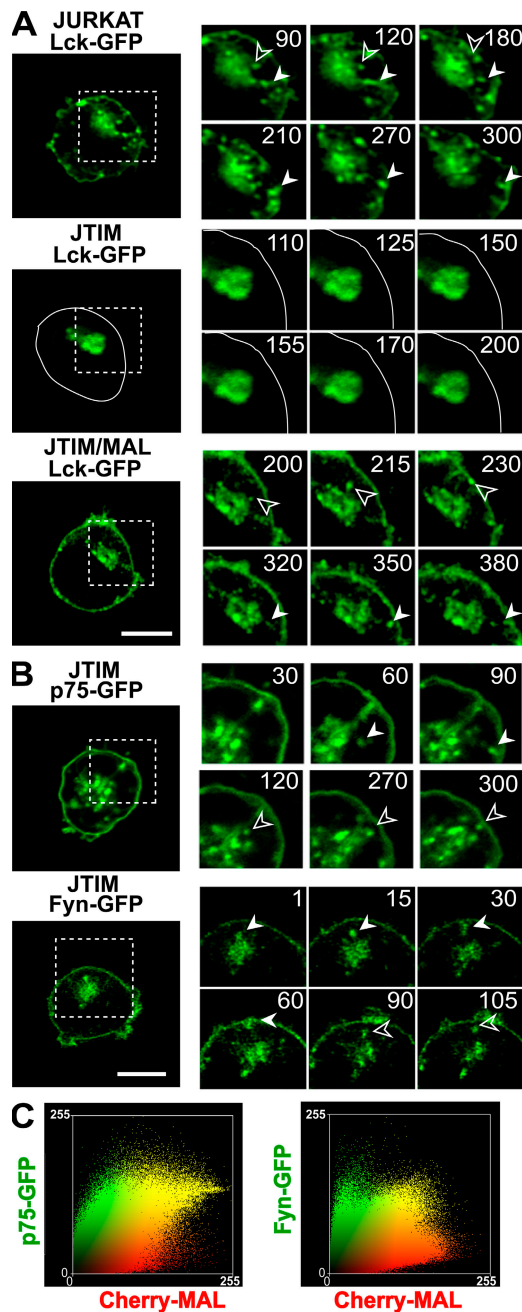


Figure 6. MAL is required for formation of vesicles transporting Lck to the plasma membrane. (A) WT Jurkat cells, JTIM cells, or JTIM/MAL cells were transiently transfected with plasmid DNA expressing Lck-GFP and monitored by time-lapse videomicroscopy to detect the formation of Lck-containing transport vesicles. The contour of the JTIM cell transfected with Lck-GFP has been drawn with a continuous line to indicate the position of the plasma membrane. (B) A similar analysis was done in JTIM cells transiently expressing p75-GFP and Fyn-GFP. The processes occurring within the regions indicated by the dashed squares are shown at higher magnification on the right. Filled and empty arrowheads indicate vesicles transporting Lck, p75, or Fyn. Numbers indicate time in seconds. Bars, 5 μ m. (C) Jurkat cells stably expressing Cherry-MAL were transiently transfected with plasmid DNA expressing p75-GFP or Fyn-GFP and subjected to time-lapse videomicroscopy. Colocalization plots of MAL

MAL defect in JTIM cells. Collectively, the results in Fig. 7 show that the sole expression of MAL in JTIM cells is sufficient to restore the signaling pathways controlling transcriptional activation of the IL-2 promoter.

DISCUSSION

The use of siRNA silencing techniques both in Jurkat and primary T cells and the isolation of a Jurkat cell variant lacking MAL expression allowed us to address the role and mechanism of action of MAL in T cells. Conjugates with APC were efficiently formed using MAL-depleted T cells, but TCR, Lck, ZAP-70, and PKC- θ did not redistribute to the IS. The requirement for MAL for IS formation was confirmed in T cell-APC conjugates formed in the presence of the SEB superantigen or a specific HA peptide. In addition to deficient IS formation, MAL-depleted cells were unable to activate signaling pathways leading to up-regulation of IL-2 promoter transcription in response to SEE and showed reduced levels of Lck at the cell periphery. All these defects were corrected by exogenous expression of MAL. Therefore, our results establish the requirement for MAL in the processes of IS formation and T cell activation.

Given the crucial role of MAL as an element of the specialized machinery for apical transport in epithelial cells (12–14, 23), an obvious aspect of interest concerning MAL function in T cells was its involvement in specialized membrane trafficking to the cell surface (15, 24). During our search for abnormally distributed plasma membrane proteins in MAL-deficient cells, we found that although Lck was distributed at both the cell periphery and in endosomes in normal Jurkat cells, Lck was practically absent from the plasma membrane and instead was concentrated in a compact intracellular structure in Jurkat cells lacking MAL expression. It is of particular note that Lck distributed normally when MAL levels were reconstituted by exogenous expression. Consistent with these findings, knockdown of MAL levels in primary T cells reduced the presence of Lck at the plasma membrane with concomitant intracellular accumulation compared with the exclusive peripheral expression of Lck in control cells. Therefore, MAL appears to be crucial for normal targeting of Lck to the T cell surface.

Lck is known to rely on membrane-trafficking mechanisms for targeting to the cell surface (6). Expression of Lck at the plasma membrane is essential for T cell function because Lck mutants that are unable to reach the plasma membrane are defective in T cell signaling (7). The presence of a pool of Lck in endosome structures and their colocalization with MAL in normal Jurkat cells are consistent with a possible role for MAL in Lck exocytosis. This view was supported by our observations of time-lapse videomicroscopy in living cells, in which Lck and MAL traveled in the same vesicles

and p75 or Fyn throughout the time-lapse experiment are shown. Pearson's correlation coefficients were 0.710 and 0.752 for MAL/p75 and MAL/Fyn, respectively.

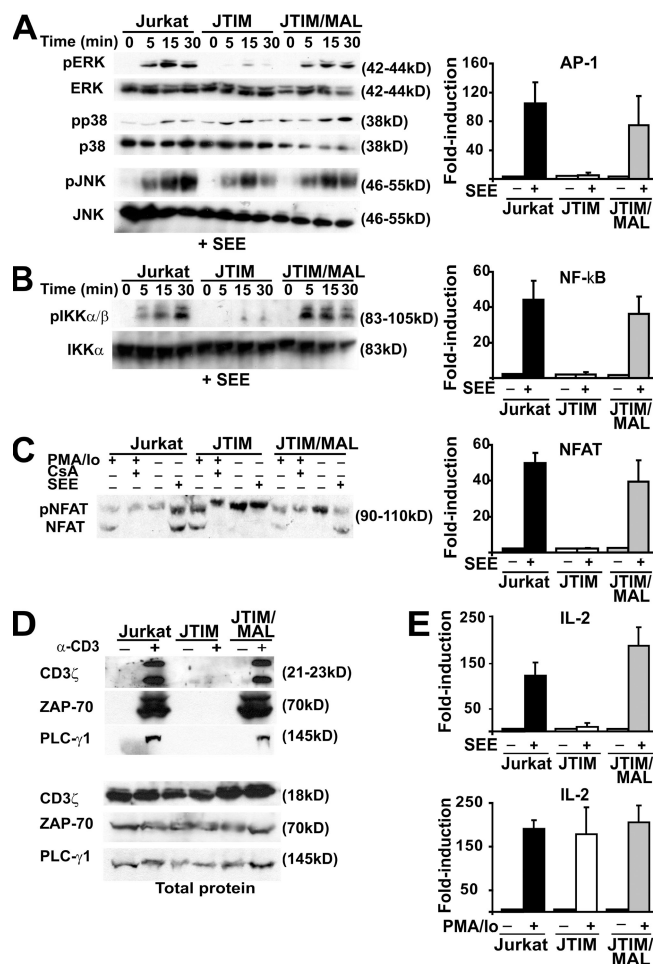


Figure 7. Signaling pathways of Jurkat cells leading to activation of AP-1, NF-κB, and NFAT and to induced tyrosine phosphorylation are dependent on MAL expression. (A) The three types of Jurkat cell were conjugated to APCs pulsed with SEE for the indicated times. Cell extracts were analyzed by immunoblotting to detect the activated, phosphorylated (p) forms or the total content of Erk, p38, and JNK as indicated (left). Cells were transfected with a luciferase reporter plasmid whose transcription was controlled by AP-1. Cells were then conjugated to APCs, which were pulsed or not with SEE. After 4 h, luciferase activity was measured (right). (B) The three types of Jurkat cell were conjugated for the indicated times to APCs pulsed with SEE. Cell extracts were analyzed by immunoblotting to detect the activated phosphorylated forms of IKK-α/β or the total content of IKK-α (left). Cells were transfected with a luciferase reporter plasmid whose transcription was controlled by NF-κB. Cells were then conjugated to APCs, which were pulsed or not with SEE. After 4 h, luciferase activity was measured (right). (C) Cells were conjugated to APCs pulsed with SEE for 1 h at 37°C. Cell extracts were analyzed by immunoblotting with anti-NFAT antibodies that detect both the inactive phosphorylated NFAT and the active dephosphorylated NFAT forms. Control of cells treated for 1 h with PMA plus ionomycin (Io) in the absence or presence of cyclosporin A (CsA) was included to help identification of phosphorylated and dephosphorylated NFAT (left). The three types of Jurkat cell were transfected with a luciferase reporter plasmid whose transcription was controlled by NFAT. Cells were then conjugated to APCs, which were pulsed or not with SEE. After 4 h, luciferase activity was measured (right). (D) Cells were treated or not with activating anti-CD3 UCHT1 antibodies for 15 min. Cell extracts were immunoprecipitated with

destined for the cell surface. The vesicles were large and formed discontinuously. It is worth noting that the formation of the vesicles containing Lck was impaired in the MAL-deficient Jurkat variant, and only a few much smaller vesicles were sporadically formed. The absence of MAL did not provoke a general block on the generation of transport vesicles because vesicles containing Fyn-GFP or p75-GFP formed efficiently in JTIM cells. Our results indicate that MAL mediates a specialized route of transport in T cells that is used for targeting Lck to the plasma membrane.

Membrane microdomains were originally postulated as being specialized platforms for apical transport (8). Although controversial (25), it is sometimes assumed that the membrane fraction resistant to detergent solubilization is enriched in membrane microdomains (26, 27). Approximately 30–50% of Lck is isolated in detergent-insoluble membrane fractions (28, 29). Consistent with the observed colocalization of MAL and Lck in endosome structures in Jurkat cells, both proteins cofractionate in a detergent-insoluble subendosomal membrane fraction (11). It is of particular note that the inability of Lck to reach the plasma membrane in MAL-deficient Jurkat cells is associated with its exclusion from detergent-insoluble membrane fractions. Similar to the strict link between plasma membrane targeting and detergent insolubility for Lck found in WT, MAL-deficient, and MAL-reconstituted Jurkat cells, polarized apical targeting of HA in Mardin-Darby canine kidney cells is associated with HA insolubility in a MAL expression-dependent manner (12). This latter observation, together with the association found between MAL and HA, was interpreted as meaning that one of MAL's functions is to recruit HA to membrane platforms for apical exocytosis (12, 20). Consistent with this view, the transport defect observed for Lck in the absence of MAL expression may be explained by a membrane alteration that prevents incorporation of Lck into specific membrane platforms acting in Lck exocytosis. Because MAL associates with Lck and exogenous expression of MAL fully restored not only the blocking of the partitioning into detergent-insoluble membranes but also the transport of Lck, it might be that a primary function of MAL in T cells is to recruit Lck to specialized membranes involved in the formation of transport carriers and the subsequent targeting of Lck to the plasma membrane.

In addition to the redistribution of receptors and signaling machinery, IS formation implies recruitment of actin

antiphosphotyrosine PY20 mAb coupled to agarose. The phosphotyrosine immunoprecipitates were immunoblotted to detect tyrosine phosphorylated CD3ζ, ZAP-70, and PLC-γ1 (top). The original extracts were immunoblotted to show the total content of CD3ζ, ZAP-70, and PLC-γ1 (bottom). (E) The three types of Jurkat cell were transiently transfected with plasmid DNA containing the luciferase gene under the control of the IL-2 promoter. After 16 h, cells were conjugated to APCs, which were pulsed or not with SEE (top), or incubated or not with PMA plus ionomycin (Io; bottom). After 4 h, cell extracts were used to determine luciferase activity. Data are represented as mean ± SEM of the luciferase activity in stimulated cells relative to that in unstimulated cells.

cytoskeleton elements, which form a specialized network of actin filaments while retaining their apparently normal subcortical organization in the rest of the cell membrane, and repositioning of MTOC, which controls the position of the secretory and endocytic compartments toward the IS (30). Repositioning of these compartments could have consequences on the activation process that could bring Fyn, Pyk2, and other signaling molecules closer to IS (31). It has also been reported that a pool of Lck and LAT that is associated with recycling endosomes translocates to mature synapses (32, 33). Therefore, the absence of MTOC reorientation in MAL-deficient cells probably affects polarized targeting from the secretory/endocytic compartments to IS (32–34).

Both actin and talin redistributed to the IS regardless of whether MAL was expressed, implying that MAL is not required for this process. Remarkably, unlike the TCR, which required MAL for IS targeting, ICAM-3 was normally recruited in the absence of MAL. This indicates that ICAM-3 targeting to IS takes place by MAL-independent mechanisms that are most probably linked to the actin cytoskeleton rearrangement. In this regard, association of ICAM-3 with ERM proteins has been previously documented (35). In contrast to the remodeling of the actin cytoskeleton, the MTOC did not reorient to the IS in the absence of MAL. MTOC reorientation is impaired in Lck- or ZAP-70-deficient Jurkat cells (36) and requires phosphorylation in tyrosine of immunoreceptor tyrosine-based activation motifs that are present at the cytoplasmic tail of the CD3 subunits (37). To analyze whether the absence of Lck at the plasma membrane can by itself fully account for the failure to trigger the signals required for proper IS formation, we forced the expression of Lck at the plasma membrane by expression of CD4/Lck and LAT/Lck transmembrane chimeras in JTIM cells. It is of particular note that the chimeras were able to restore the targeting of TCR, ZAP-70, and PKC- θ to IS, indicating that these transmembrane forms of Lck, regardless of their level of partitioning into detergent-insoluble membranes, were equally able to initiate TCR-induced signaling even in the absence of MAL expression. Despite this, however, both chimeras did not correct MTOC reorientation or TCR-induced downstream signaling events such as ERK activation and CD69 up-regulation. These findings indicate that the deficient targeting of Lck to the plasma membrane is not the sole cause of the effects observed in MAL-deficient cells and implies that, in addition to transporting Lck, MAL mediates other functions in the cell, probably related to the transport of other specific molecules and the repositioning of the MTOC.

Jurkat cells lacking MAL expression were unable to activate transcription of the IL-2 promoter in response to stimulation with SEE. Consistent with this observation, the signaling pathways leading to activation of transcription factors AP-1, NF- κ B, and NFAT, or to increased tyrosine phosphorylation of specific substrates, were defective. Reconstitution of MAL levels by exogenous expression made these pathways fully operative and rescued normal response of the IL-2 promoter to T cell stimulation. Restoration of these pathways is proba-

bly mediated by correction of the abnormal targeting of Lck, and probably of other signaling molecules, that is observed in the absence of MAL expression.

A constitutive MAL KO mouse line was generated to investigate the role of MAL on myelin formation (38). The mice were viable, had a normal life span, and appeared grossly normal. However, a closer inspection revealed defects in axon–glia interactions. Importantly, although MAL is expressed in oligodendrocytes and Schwann cells, alterations were observed only in the central nervous system, whereas the peripheral nervous system did not seem to be affected. The possible existence of a compensatory mechanism of another as yet unknown MAL family protein was claimed that might replace the functional role of endogenous MAL at the peripheral nervous system. Unlike humans, thymus, primary T cells, and T cell lines of mouse origin do not express the MAL gene. The most plausible explanation is that another member of the MAL protein family or of the MARVEL domain-containing protein superfamily does the job in mouse T cells. This reminds us of the caution that must be exercised in making definitive assignments of physiological function across species. Although animal models are undoubtedly quite useful for biomedical research, it is clear that studies in human cells need to be performed to learn about human cell functioning.

Progress in understanding MAL function as a component of the machinery for specialized routes of protein transport was first made possible in epithelial cells by taking advantage of the seminal discoveries made in epithelial cells concerning protein sorting (39). In this study, using gene silencing in Jurkat T cells and primary human T lymphocytes, and a Jurkat cell clone with deficient MAL expression, we have found an essential role for MAL in exocytic transport of Lck to the plasma membrane. In addition, our results highlight the similarity of the Lck transport process of T cells to that of the specialized MAL-mediated apical route of protein exocytosis of polarized epithelial cells. Normal functioning of this novel transport pathway is essential for T cell activation and IS formation.

MATERIALS AND METHODS

Materials. Rabbit antibodies to CD3 ζ and ZAP-70, and mAb UCHT-1 (IgG1) and APA 1.1 to CD3 (used for cell activation and immunoblot analysis, respectively), were provided by A. Alarcón (Centro de Biología Molecular “Severo Ochoa”, Madrid, Spain). Rabbit polyclonal antibody to Lck (used for immunofluorescence analysis) was provided by A. Veillette (McGill University, Montreal, Canada). Mouse mAb MEM-43/5 to CD59 was a gift from V. Horejsi (Institute of Molecular Genetics, Prague, Czech Republic); mAbs to PLC- γ 1 and PKC- θ and the antiphosphotyrosine PY20 antibodies, coupled or not to agarose, were obtained from BD; mouse hybridomas producing anti-CD3 ϵ mAb OKT3 and anti-Myc mAb 9E10 were purchased from the American Type Culture Collection; and antibodies to LAT were obtained from Millipore. Antibodies to total or phosphorylated Erk and p38 used for immunoblotting were obtained from Promega and Santa Cruz Biotechnology, Inc., respectively. The anti-JNK and anti-IKK- α/β antibodies were purchased from Cell Signaling Technology. The antibodies to NFAT, ICAM-3, and mouse CD4 were provided by J.M. Redondo (Centro de Biología Molecular “Severo Ochoa”, Madrid, Spain), F. Sánchez-Madrid (Hospital de la Princesa, Madrid, Spain), and J.M. Rojo (Centro de Investigaciones Biológicas, Madrid, Spain), respectively. Antibodies to γ -tubulin, talin, and GFP were obtained from Sigma-Aldrich. We

obtained SEE and SEB from Toxin Technology, Inc. HRP-conjugated antibodies were obtained from Thermo Fisher Scientific. Fluorochrome-labeled secondary goat antibodies, fluorescent phalloidin, and the fluorescent cell tracker chloromethyl derivative of aminocoumarin (CMAC) were purchased from Invitrogen.

Cell culture conditions and conjugate formation procedure. Human T lymphoblastoid Jurkat cells were grown in RPMI 1640 supplemented with 5% FBS (Sigma-Aldrich), 50 U/ml penicillin, and 50 µg/ml streptomycin at 37°C in an atmosphere of 5% CO₂/95% air. To distinguish Raji cells from Jurkat cells in the conjugates, Raji cells (3.0×10^6 cells/ml) were preincubated with 10 µM CMAC for 20 min at 37°C, washed, and resuspended in RPMI/5% FBS. The cells were then incubated for 20 min in the presence or absence of 4 µg/ml SEE and mixed with an equal number of Jurkat cells (5.0×10^5 cells/well) in a final volume of 50 µl, incubated at 37°C for 15 min, and plated onto poly-L-lysine-coated slides. After incubation for 15 min at 37°C, cells were fixed with formalin, permeabilized or not, blocked with 3% BSA and 100 µg/ml γ-globulin, and stained with the appropriate antibodies. Jurkat CH7C17 cells (21) expressing exogenous TCR-α and TCR-β (Vβ3) chains specific for HA were conjugated to HOM2 cells in the presence of 200 µg/ml HA peptide 307–319 (PKYVKQNTLKLAT), a control inactive peptide (PKYVKQNTLELAT), or 4 µg/ml SEB. For conjugation of primary T cells, freshly isolated T lymphocytes from healthy donors were incubated with SEE-pulsed Raji cells and processed as described for the Jurkat-APC conjugates. The experiments with human cells were done according to the guidelines of the Bioethics Committee of the Spanish Research Council and were approved by the institutional Management Committee of the Centro de Biología Molecular “Severo Ochoa”.

DNA constructs and transfection conditions. The 5′-TCATG-GCCCCGCGAGCGGC-3′ and 5′-GGGAGCTTGCTGTGTCTAA-3′ sequences, which target the sequences surrounding the AUG translation initiation site and the 3′ untranslated region of MAL mRNA, respectively, separated by a short spacer (5′-TTCAAGAGA-3′) from their reverse complement, were cloned under the control of the H1-RNA promoter in the pSUPER DNA vector (40) thereby originating the pMAL-siRNA1 and pMAL-siRNA2 constructs. These plasmids were then modified by insertion of a DNA fragment containing the GFP coding sequence under the control of the CMV immediate-early promoter generating the pMAL-siRNA1/GFP and pMAL-siRNA2/GFP constructs. A similar construct containing a target-recognition sequence corresponding to BENE mRNA, which is not expressed in T cells (41), was used as a control. The DNA constructs expressing the ectodomain and transmembrane region of mouse CD4 fused to Lck (CD4/Lck) (42) or to GFP (CD4ΔCyt-GFP) (43) were gifts from A. Weiss (University of San Francisco, San Francisco, CA) and M.F. Krummel (University of San Francisco, San Francisco, CA), respectively. The CD4/Lck construct was used to generate a LAT/Lck construct by excising the CD4 sequences and substituting them by the LAT sequences encoding the first 36 aa of the amino terminus of LAT, which included its extracellular and transmembrane domains. Sequences encoding the c-Myc tag were finally added to the LAT/Lck coding sequence. The plasmid expressing p75-GFP in pEGFP-N1 (44) was a gift from E. Rodriguez-Boulan (Cornell University, Ithaca, NY). The Fyn-GFP construct (45) and the Lck₁₀-GFP construct expressing the first 10-aa sequence of Lck fused to the amino terminus of GFP (46) were generously provided by N. Yamaguchi (Chiba University, Chiba, Japan) and W. Rodgers (Oklahoma Medical Research Foundation, Oklahoma City, OK), respectively. The DNA constructs expressing GFP or Cherry appended to the carboxyl terminus of Lck (Lck-GFP and Lck-Cherry) or the amino terminus of MAL (GFP-MAL and Cherry-MAL) were made by standard techniques. Jurkat cells and primary human T cells were transfected by electroporation using the Gene Pulser system (Bio-Rad Laboratories). As controls of the siRNA experiments, we used Jurkat cells stably expressing N-terminal Myc-tagged MAL proteins with either an intact (RWKSS, MAL/myc) or a modified (RWSSS, MALmut/myc) MAL carboxyl terminus encoded by mRNAs that do not fully pair with the MAL siRNA used (20).

Generation, characterization, and reconstitution of a Jurkat cell mutant defective in MAL expression. The JTIM cell line was generated by chemical mutagenesis using methanesulfonic acid ethyl ester (EMS; Sigma-Aldrich) and selection for clones that were defective in TCR-induced signaling in a manner that is similar to that previously described for PMA-induced up-regulation (19). The deficiency in MAL was identified by a comparison of genes expressed in parental Jurkat and JTIM using DNA microarrays, as described for other mutant Jurkat cell lines (18). JTIM cells were provided by A. Weiss (University of San Francisco, San Francisco, CA). Sometimes the JTIM cells were suddenly able to recover MAL expression spontaneously in a manner that could not be controlled. This probably involves changes in the methylation state of the MAL gene because treatment with the demethylating agent 5-aza-2′-deoxycytidine is able to recover MAL gene expression in these cells (unpublished data) as well as in certain tumor cells in which the MAL gene is silent (47). To circumvent this problem, the absence of MAL expression was checked in parallel by immunoblotting to validate all the experiments done with JTIM cells.

To reconstitute expression with exogenous MAL, JTIM cells were transfected with a pCR3.1 DNA construct (Invitrogen) containing a 0.8-kb EcoRI-XhoI MAL cDNA fragment, which encompasses the 5′ untranslated region, the entire MAL coding region, and part of the 3′ untranslated sequences of MAL mRNA. After selection with 1 mg/ml G-418 sulfate for at least 6 wk after transfection, drug-resistant cell clones were screened for MAL expression by immunoblot analysis with anti-MAL mAb 6D9. All the reconstituted clones that were obtained expressed MAL at similar levels. The cell clones positive for MAL expression were thereafter maintained in drug-free medium. Although all the results presented in this contribution were obtained using the same JTIM/MAL cell clone, two other reconstituted clones were analyzed to confirm our main findings. Jurkat cells stably expressing MAL/myc, MALmut/myc, or GFP-MAL were generated according to a similar protocol.

Flow cytometry. For analysis of CD69 up-regulation, Jurkat cells and JTIM cells were transfected with pEGFP and, in the case of JTIM cells, cotransfected or not with the chimeras expressing CD4/Lck or LAT/Lck. After 24 h, cells were stimulated or not with 10 µg/ml of anti-CD3 antibodies or 50 ng/ml PMA. The GFP-expressing cell population was analyzed 16 h later for the expression of surface CD69 with fluorescent anti-CD69 antibodies (Invitrogen) in a FACSCalibur flow cytometer using CellQuest Pro software (BD). For analysis of Erk phosphorylation, normal Jurkat cells and JTIM cells were transfected with CD4ΔCyt-GFP and, in the case of JTIM cells, cotransfected or not with the chimeras expressing CD4/Lck or LAT/Lck. After 24 h, cells were stimulated or not with anti-CD3 antibodies or PMA for 15 min and then were fixed with 2% paraformaldehyde and permeabilized with methanol at −20°C. Phosphorylated Erk was analyzed in the cell population expressing CD4ΔCyt-GFP using anti-phospho-Erk rabbit antibodies (Cell Signaling Technology) and a secondary fluorescent anti-rabbit Ig antibody. The use of CD4ΔCyt-GFP facilitates the identification of the transfected cell population as the fluorescence of this transmembrane chimera is retained in fixed permeabilized cells to a greater extent than using just GFP. The cotransfection efficiency was >80% as determined by immunofluorescence microscopy. The mean fluorescence intensity obtained in each case for CD69 or phospho-Erk was compared with that obtained for normal Jurkat cells stimulated with anti-CD3 antibodies, which was taken as 100%. Controls to assess the specificity of the labeling included incubations with control primary antibodies or omission of the primary antibodies.

Luciferase reporter assays. Jurkat cells were transiently transfected using Lipofectamine (Promega) with plasmid DNA (150 ng/1.0 × 10⁶ cells) containing the firefly luciferase gene under the control of IL-2 promoter, AP-1, NF-κB, or NFAT responsive elements and with a renilla luciferase reporter plasmid (Promega). Jurkat cells were then conjugated with Raji B cells in the presence or absence of SEE for 4 h or activated with anti-CD3 antibodies or with 20 ng/ml PMA plus 5 µM ionomycin for 4 h. Aliquots of cell lysates were analyzed for luciferase activity with the Dual Luciferase Reporter Assay kit according to the manufacturer's protocol (Promega). The protein

content in the extracts was determined with a protein assay kit (Bio-Rad Laboratories). All experiments were done three times, each with three replicates. Results are represented as mean \pm SEM of the luciferase activity in stimulated cells relative to that in unstimulated cells.

Detergent extraction procedures, immunoblotting, and immunoprecipitation analyses. Jurkat cells (5.0×10^7 cells) were lysed for 15 min in 25 mM Tris-HCl, pH 7.2, 150 mM NaCl, and 0.2% Triton X-100 at 4°C in the presence of phosphatase and protease inhibitors. The extract was brought to 40% sucrose (wt/wt) and placed at the bottom of two sequential layers of 30 and 5% sucrose. Gradients were centrifuged to equilibrium, and the soluble and low-density insoluble fractions were harvested (48). Equivalent aliquots from the soluble and insoluble fractions were subjected to SDS-PAGE and transferred to Immobilon-P membranes (Millipore). After blocking with 5% nonfat dry milk and 0.05% Tween-20 in PBS, blots were incubated with the appropriate antibodies for 1 h. After several washings, blots were incubated for 30 min with secondary antibodies coupled to HRP and developed using a commercial kit (GE Healthcare). For immunoprecipitation studies, cells were lysed in 25 mM Tris-HCl, pH 7.4, 150 mM NaCl, 5 mM EDTA, 0.5% Triton X-100, and a cocktail of phosphatase and protease inhibitors. The lysates were precleared for 1 h at 4°C with protein G-Sepharose, centrifuged, and the supernatant was incubated with the indicated specific antibodies for 1 h at 4°C. After incubation with protein G-Sepharose for 1 h, the immunoprecipitates were collected by centrifugation, washed six times, and analyzed by immunoblotting with the appropriate antibodies.

Immunofluorescence and time-lapse confocal microscopic analyses. Cells were fixed in formalin for 20 min, rinsed, and treated with 10 mM glycine in PBS for 5 min to quench the aldehyde groups. Cells were then washed, permeabilized or not with 0.2% Triton X-100 in PBS at 4°C for 5 min, rinsed, incubated with 3% (wt/vol) BSA for 15 min, and incubated with the primary antibody. After 1 h at room temperature, cells were washed and incubated with the appropriate fluorescent secondary antibody. For double-labeling experiments, the same procedure was repeated for the second primary antibody. In the cases where two different mouse mAbs were used, the analysis was done using compatible fluorochrome-labeled isotype-specific secondary antibodies. Controls to assess the specificity of the labeling included incubations with control primary antibodies and omission of the primary antibodies. Images were obtained using a confocal laser microscope (Meta LSM 510; Carl Zeiss, Inc.). For the quantitative analysis of Lck distribution, the Lck fluorescence signal was profiled along a line at the equatorial plane of the cell using the Image J program (National Institutes of Health; <http://rsb.info.nih.gov/ij/index.html>). The ratio of internal to plasma membrane fluorescence was calculated for each type of Jurkat cell in three independent experiments ($n = 20$ cells of each type). Cells with a ratio greater than or equal to the mean number of normal Jurkat cells + $1.5 \times$ SEM were considered to express low levels of Lck at the plasma membrane. Only 5% of WT Jurkat cells met this criterion. For single-color time-lapse confocal fluorescence microscopy, normal Jurkat cells, JTIM cells, or JTIM/MAL were transfected with Lck-GFP, p75-GFP, or Fyn-GFP. For dual-color time-lapse microscopy, normal Jurkat cells stably expressing GFP-MAL or Cherry-MAL were used for the expression of Cherry (Lck) or GFP (p75, Fyn) constructs, respectively. 24 h after transfection, cells were plated onto fibronectin-coated chambers and maintained at 37°C. Images were captured every 15 s using a confocal microscope (LSM 510; Carl Zeiss, Inc.) equipped with a 63 \times lens with a 1.4 NA oil immersion objective and transferred to a computer workstation running MetaMorph imaging software (MDS Analytical Technologies). For deconvolution we used Huygens 3.0 software (Scientific Volume Imaging), and colocalization graphics were produced with Image J. Videos are displayed at three frames/second.

Online supplemental material. Fig. S1 shows a characterization of the Jurkat cell variant deficient in MAL expression. Fig. S2 shows that MAL is required for translocation of ZAP-70 and LAT to IS. Fig. S3 shows a pulse-chase analysis analyzing the incorporation of Lck to detergent-insoluble or

total membrane fractions. Video 1 shows time-lapse microscopy showing MAL and Lck in the same transport carriers destined for the plasma membrane. Videos 2–4 show time-lapse microscopy of Lck in Jurkat, JTIM, and JTIM/MAL cells, respectively. Videos 5 and 6 show time-lapse microscopy of p75 and Fyn, respectively, in JTIM cells. Online supplemental material is available at <http://www.jem.org/cgi/content/full/jem.20080552/DC1>.

We thank A. Weiss, M. Tomlinson, and T. Finco for providing the JTIM cell variant and helpful comments. We thank S. Gómez and A. Jiménez for technical help and Max Diehn and Pat Brown (Stanford University) for help with microarray analysis in the initial studies of JTIM cells. The expert technical advice of C.C. Combs and D. Malide of the Light Microscopy Facility of the National Institutes of Health (Bethesda, Maryland) on the time-lapse experiments and image processing and of C. Sánchez, T. Villalba, and V. Labrador of the Optical and Confocal Microscopy Unit of the Centro de Biología Molecular "Severo Ochoa" are also acknowledged. We are grateful to F. Sánchez-Madrid, B. Alarcón, and F. Martín-Belmonte for their helpful advice and sharing of materials throughout this study.

This work was supported by grants from the Ministerio de Educación y Ciencia, Spain (BFU2006-01925 to M.A. Alonso) and from the Intramural Research Program of the National Institutes of Health, National Heart, Lung, and Blood Institute (NHLBI; to R. Puertollano). An institutional grant from the Fundación Ramón Areces to Centro de Biología Molecular "Severo Ochoa" is also acknowledged.

The authors declare no competing financial interests.

Submitted: 14 March 2008

Accepted: 31 October 2008

REFERENCES

- Lin, J., and A. Weiss. 2001. T cell receptor signalling. *J. Cell Sci.* 114:243–244.
- Karnitz, L., S.L. Sutor, T. Torigoe, J.C. Reed, M.P. Bell, D.J. McKean, P.J. Leibson, and R.T. Abraham. 1992. Effects of p56lck deficiency on the growth and cytolytic effector function of an interleukin-2-dependent cytotoxic T-cell line. *Mol. Cell. Biol.* 12:4521–4530.
- Straus, D.B., and A. Weiss. 1992. Genetic evidence for the involvement of the Lck tyrosine kinase in signal transduction through the T cell antigen receptor. *Cell* 70:585–593.
- Ley, S.C., M. Marsh, C.R. Bebbington, K. Proudfoot, and P. Jordan. 1994. Distinct intracellular localization of Lck and Fyn protein tyrosine kinases in human T lymphocytes. *J. Cell Biol.* 125:639–649.
- Shenoy-Scaria, A.M., L.K. Gauen, J. Kwong, A.S. Shaw, and D.M. Lublin. 1993. Palmitoylation of an amino-terminal cysteine motif of protein tyrosine kinases p56lck and p59fyn mediates interaction with glycosylphosphatidylinositol-anchored proteins. *Mol. Cell. Biol.* 13:6385–6392.
- Bijlmakers, M.-J.J.E., and M. Marsh. 1999. Trafficking of an acylated cytosolic protein: newly synthesized p56^{lck} travels to the plasma membrane via the exocytic pathway. *J. Cell Biol.* 145:457–468.
- Kabouridis, P.S., A.I. Magee, and S.C. Ley. 1997. S-acylation of LCK protein tyrosine kinase is essential for its signalling function in T lymphocytes. *EMBO J.* 16:4983–4998.
- Simons, K., and A. Wandinger-Ness. 1990. Polarized sorting in epithelia. *Cell* 62:207–210.
- Sanchez-Pulido, L., F. Martín-Belmonte, A. Valencia, and M.A. Alonso. 2002. MARVEL: a conserved domain involved in membrane apposition events. *Trends Biochem. Sci.* 27:599–601.
- Alonso, M.A., and S.M. Weissman. 1987. cDNA cloning and sequence of MAL, a hydrophobic protein associated with human T-cell differentiation. *Proc. Natl. Acad. Sci. USA* 84:1997–2001.
- Millán, J., and M.A. Alonso. 1998. MAL, a novel integral membrane protein of human T lymphocytes, associates with glycosylphosphatidylinositol-anchored proteins and Src-like tyrosine kinases. *Eur. J. Immunol.* 28:3675–3684.
- Puertollano, R., F. Martín-Belmonte, J. Millán, M.C. de Marco, J.P. Albar, L. Kremer, and M.A. Alonso. 1999. The MAL proteolipid is necessary for normal apical transport and accurate sorting of the influenza virus hemagglutinin in Madin-Darby canine kidney cells. *J. Cell Biol.* 145:141–151.
- Cheong, K.H., D. Zacchetti, E.E. Schneeberger, and K. Simons. 1999. VIP17/MAL, a lipid raft-associated protein, is involved in apical transport in MDCK cells. *Proc. Natl. Acad. Sci. USA* 96:6241–6248.

14. Martin-Belmonte, F., R. Puertollano, J. Millan, and M.A. Alonso. 2000. The MAL proteolipid is necessary for the overall apical delivery of membrane proteins in the polarized epithelial Madin-Darby canine kidney and Fischer rat thyroid cell lines. *Mol. Biol. Cell.* 11:2033–2045.
15. Alonso, M.A., and J. Millán. 2001. The role of lipid rafts in signalling and membrane trafficking in T lymphocytes. *J. Cell Sci.* 114:3957–3965.
16. Huppa, J.B., and M.M. Davis. 2003. T-cell-antigen recognition and the immunological synapse. *Nat. Rev. Immunol.* 3:973–983.
17. Abraham, R.T., and A. Weiss. 2004. Jurkat T cells and development of the T-cell receptor signalling paradigm. *Nat. Rev. Immunol.* 4:301–308.
18. Roose, J.P., M. Diehn, M.G. Tomlinson, J. Lin, A.A. Alizadeh, D. Botstein, P.O. Brown, and A. Weiss. 2003. T cell receptor-independent basal signaling via Erk and Abl kinases suppresses RAG gene expression. *PLoS Biol.* 1:E53.
19. Roose, J.P., M. Mollenauer, V.A. Gupta, J. Stone, and A. Weiss. 2005. A diacylglycerol-protein kinase C-RasGRP1 pathway directs Ras activation upon antigen receptor stimulation of T cells. *Mol. Cell. Biol.* 25:4426–4441.
20. Puertollano, R., J.A. Martinez-Menarguez, A. Batista, J. Ballesta, and M.A. Alonso. 2001. An intact dilysin-like motif in the carboxyl terminus of MAL is required for normal apical transport of the influenza virus hemagglutinin cargo protein in epithelial Madin-Darby canine kidney cells. *Mol. Biol. Cell.* 12:1869–1883.
21. Hewitt, C.R., J. Lamb, J. Hayball, M. Hill, M. Owen, and R. O’Hehir. 1992. Major histocompatibility complex independent clonal T cell anergy by direct interaction of *Staphylococcus aureus* enterotoxin B with the T cell antigen receptor. *J. Exp. Med.* 175:1493–1499.
22. Bolte, S., and F.P. Cordelières. 2006. A guided tour into subcellular colocalization analysis in light microscopy. *J. Microsc.* 224:213–232.
23. Martin-Belmonte, F., P. Arvan, and M.A. Alonso. 2001. MAL mediates apical transport of secretory proteins in polarized epithelial Madin-Darby canine kidney cells. *J. Biol. Chem.* 276:49337–49342.
24. Millan, J., M.C. Montoya, D. Sancho, F. Sanchez-Madrid, and M.A. Alonso. 2002. Lipid rafts mediate biosynthetic transport to the T lymphocyte uropod subdomain and are necessary for uropod integrity and function. *Blood.* 99:978–984.
25. Munro, S. 2003. Lipid rafts: elusive or illusive? *Cell.* 115:377–388.
26. Hancock, J.F. 2006. Lipid rafts: contentious only from simplistic standpoints. *Nat. Rev. Mol. Cell. Biol.* 7:456–462.
27. Pike, L.J. 2006. Rafts defined: a report on the Keystone symposium on lipid rafts and cell function. *J. Lipid Res.* 47:1597–1598.
28. Montixi, C., C. Langlet, A.-M. Bernard, J. Thimonier, C. Dubois, M.A. Wurbel, J.P. Chauvin, M. Pierres, and H.T. He. 1998. Engagement of T cell receptor triggers its recruitment to low density detergent-insoluble membrane domains. *EMBO J.* 17:5334–5348.
29. Xavier, R., T. Brennan, Q. Li, C. McCormack, and B. Seed. 1998. Membrane compartmentation is required for efficient T cell activation. *Immunity.* 8:723–732.
30. Billadeau, D.D., J.C. Nolz, and T.S. Gomez. 2007. Regulation of T-cell activation by the cytoskeleton. *Nat. Rev. Immunol.* 7:131–143.
31. Sancho, D., M. Vicente-Manzanares, M. Mittelbrunn, M.C. Montoya, M. Gordón-Alonso, J.M. Serrador, and F. Sánchez-Madrid. 2002. Regulation of microtubule-organizing center orientation and actomyosin cytoskeleton rearrangement during immune interactions. *Immunol. Rev.* 189:84–97.
32. Ehrlich, L.I.R., P.J.R. Ebert, M.F. Krummel, A. Weiss, and M.M. Davis. 2002. Dynamics of p56lck translocation to the T cell immunological synapse following agonist and antagonist stimulation. *Immunity.* 17:809–822.
33. Bonello, G., N. Blanchard, M.C. Montoya, E. Aguado, C. Langlet, H.-T. He, S. Nunez-Cruz, M. Malissen, F. Sanchez-Madrid, D. Olive, et al. 2004. Dynamic recruitment of the adaptor protein LAT: LAT exists in two distinct intracellular pools and controls its own recruitment. *J. Cell Sci.* 117:1009–1016.
34. Das, V., B. Nal, A. Dujancourt, M.-I. Thoulouze, T. Galli, P. Roux, A. Dautry-Varsat, and A. Alcover. 2004. Activation-induced polarized recycling targets T cell antigen receptors to the immunological synapse: involvement of SNARE complexes. *Immunity.* 20:577–588.
35. Serrador, J.M., M. Vicente-Manzanares, J. Calvo, O. Barreiro, M.C. Montoya, R. Schwartz-Albiez, H. Furthmayr, F. Lozano, and F. Sanchez-Madrid. 2002. A novel serine-rich motif in the Intercellular Adhesion Molecule 3 is critical for its Ezrin/Radixin/Moesin-directed subcellular targeting. *J. Biol. Chem.* 277:10400–10409.
36. Morgan, M.M., C.M. Labno, G.A. Van Seventer, M.F. Denny, D.B. Straus, and J.K. Burkhardt. 2001. Superantigen-induced T cell:B cell conjugation is mediated by LFA-1 and requires signaling through Lck, but not ZAP-70. *J. Immunol.* 167:5708–5718.
37. Lowin-Kropf, B., V.S. Shapiro, and A. Weiss. 1998. Cytoskeletal polarization of T cells is regulated by an immunoreceptor tyrosine-based activation motif-dependent mechanism. *J. Cell Biol.* 140:861–871.
38. Schaeren-Wiemers, N., A. Bonnet, M. Erb, B. Erne, U. Bartsch, F. Kern, N. Mantei, D. Sherman, and U. Suter. 2004. The raft-associated protein MAL is required for maintenance of proper axon-glia interactions in the central nervous system. *J. Cell Biol.* 166:731–742.
39. Rodriguez-Boulant, E., G. Kreitzer, and A. Musch. 2005. Organization of vesicular trafficking in epithelia. *Nat. Rev. Mol. Cell Biol.* 6:233–247.
40. Brummelkamp, T.R., R. Bernards, and R. Agami. 2002. A system for stable expression of short interfering RNAs in mammalian cells. *Science.* 296:550–553.
41. del Carmen de Marco, M., L. Kremer, J.P. Albar, J.A. Martínez-Menárguez, J. Ballesta, M.A. García-López, M. Marazuela, R. Puertollano, and M.A. Alonso. 2001. BENE, a novel raft-associated protein of the MAL proteolipid family, interacts with caveolin-1 in human endothelial-like ECV304 cells. *J. Biol. Chem.* 276:23009–23017.
42. Xu, H., and D.R. Littman. 1993. A kinase-independent function of Lck in potentiating antigen-specific T cell activation. *Cell.* 74:633–643.
43. Krummel, M.F., M.D. Sjaastad, C. Wulfig, and M.M. Davis. 2000. Differential clustering of CD4 and CD3z during T cell recognition. *Science.* 289:1349–1352.
44. Kreitzer, G., A. Marmorstein, P. Okamoto, R. Vallee, and E. Rodriguez-Boulant. 2000. Kinesin and dynamin are required for post-Golgi transport of a plasma-membrane protein. *Nat. Cell Biol.* 2:125–127.
45. Kasahara, K., Y. Nakayama, I. Sato, K. Ikeda, M. Hoshino, T. Endo, and N. Yamaguchi. 2007. Role of Src-family kinases in formation and trafficking of macropinosomes. *J. Cell. Physiol.* 211:220–232.
46. Van Komen, J.S., S. Mishra, J. Byrum, G.R. Chichili, J.C. Yaciuk, A.D. Farris, and W. Rodgers. 2007. Early and dynamic polarization of T cell membrane rafts and constituents prior to TCR stop signals. *J. Immunol.* 179:6845–6855.
47. Lind, G.E., T. Ahlquist, and R.A. Lothe. 2007. DNA hypermethylation of MAL: a promising diagnostic biomarker for colorectal tumors. *Gastroenterology.* 132:1631–1632.
48. Brown, D.A., and J.K. Rose. 1992. Sorting of GPI-anchored proteins to glycolipid-enriched membrane subdomains during transport to the apical cell surface. *Cell.* 68:533–544.